

---

# Supplement

1

## 2 1. Calmet model introduction

3 CALMET employs a two-step method to compute the wind field. In the first step,  
4 the initial guessed wind field is adjusted based on the kinematic impacts of terrain,  
5 blocking effects, and slope flow. The second step involves incorporating  
6 observational data into the wind field derived from step 1 using an objective  
7 analysis procedure. CALMET, as a three-dimensional microscale meteorological  
8 diagnostic model, incorporates the kinematic impacts of terrain on vertical velocity  
9 and horizontal wind components, the influence of terrain on wind field dynamics,  
10 and the thermodynamic blocking effects of terrain on wind field dynamics. The  
11 simulation of near-surface winds in the model is highly sensitive to the localized  
12 effects caused by the uneven nature of terrain and the Earth's surface.

## 13 2. Calculation method of wind shear

14 According to ICAO's recommended standards for vertical shear strength of  
15 horizontal wind, wind shear affecting aircraft is classified into four grades based on  
16 the vertical thickness of the air layer: mild (0-2 m/s/30m), moderate (2.1-4  
17 m/s/30m), strong (4.1-6 m/s/30m), and severe (above 6 m/s/30m). In this study,  
18 wind shear is computed for each layer at intervals of 10 meters (m/s/10m) for  
19 consistency in units across different altitude layers. This standardization facilitates a  
20 uniform assessment of wind shear intensity.

21 To ensure consistency in data, the wind speed in WRF is interpolated from the  
22 PH layers to the height layers of the CALMET model. This interpolation aligns the  
23 wind fields simulated by both models on the same set of vertical layers.  
24 Subsequently, the following method is employed to calculate VWS:

25 Let  $s_1$  and  $s_2$  represent the total wind speeds in the upper and lower layers,  
26 respectively. Also, let  $\theta$  denote the difference in wind direction between the upper  
27 and lower layers. The formula for calculating the vertical wind shear  $\beta$  is given by:

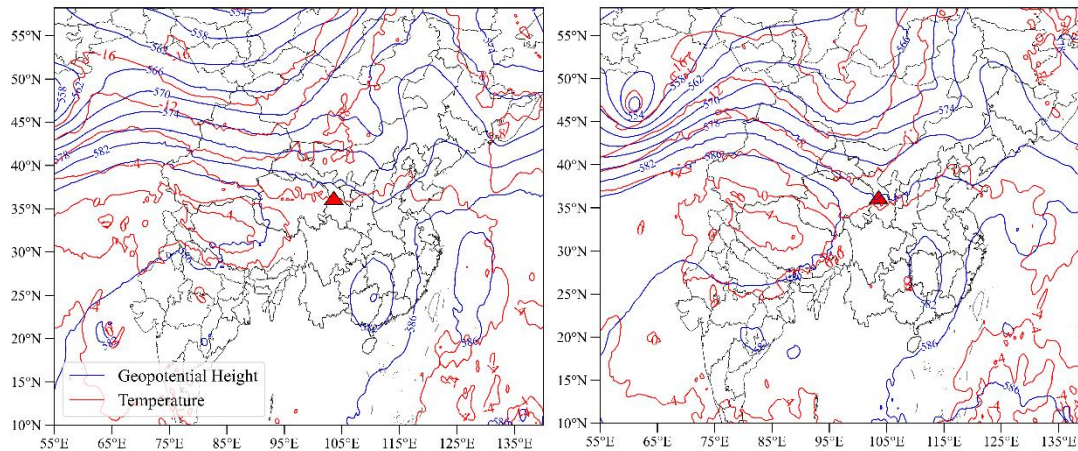
$$28 \quad \beta = \sqrt{s_1^2 + s_2^2 - 2s_1s_2\cos\theta} \quad (4)$$

29 Where:

$$s_1^2 = u_1^2 + v_1^2, s_2^2 = u_2^2 + v_2^2, \theta = |\theta_1 - \theta_2|, \theta_1 = \arctan\left(\left|\frac{u_1}{v_1}\right|\right), \theta_2 = \arctan\left(\left|\frac{u_2}{v_2}\right|\right)$$

30

### 3. Description of weather process

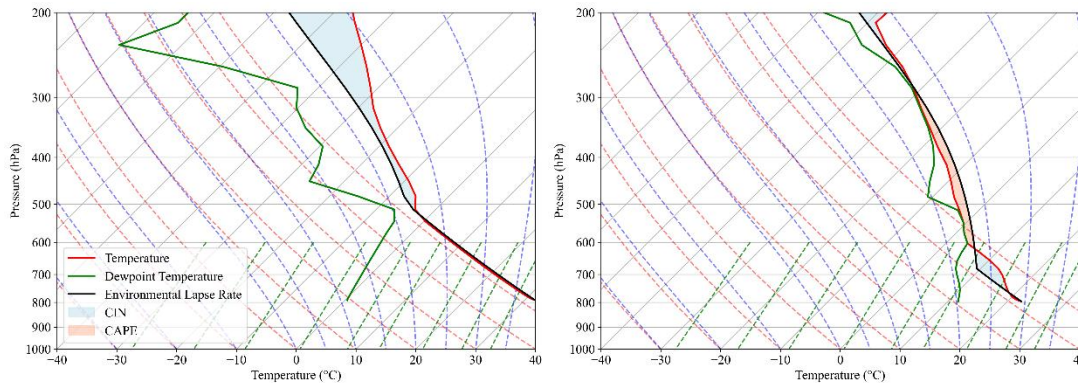


31

32

(a)

(b)



33

34

(c)

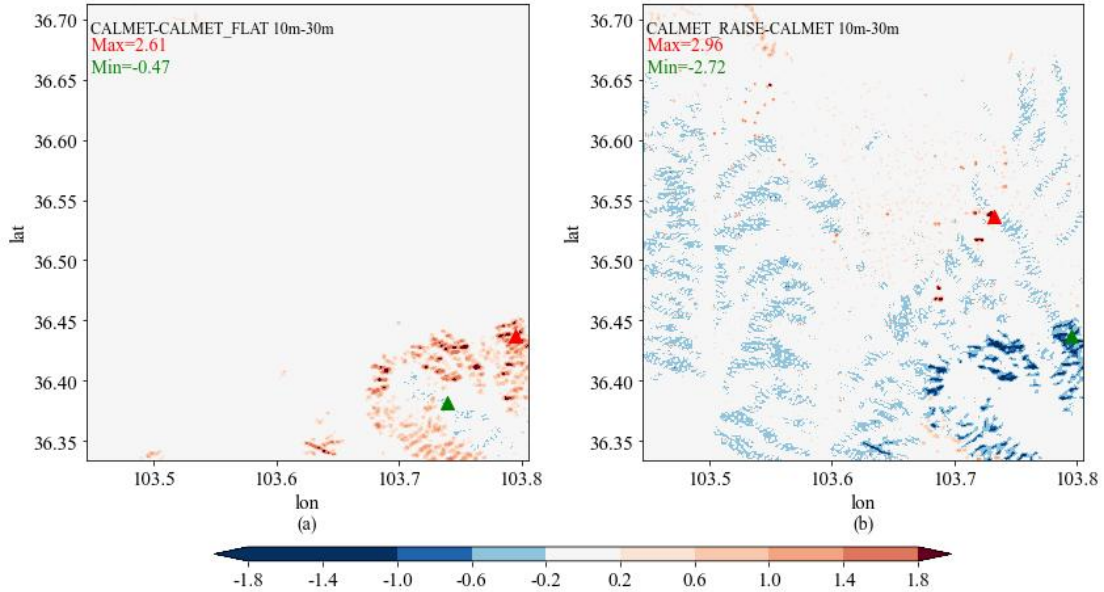
(d)

35 *Figure S1. Atmospheric Circulation Patterns at 500hPa and Skew-T Diagrams for*  
36 *Lanzhou Zhongchuan Airport on July 3, 2022, at 08:00 (a)(c) and July 4, 2022, at 08:00*  
37 *(b)(d). (a)(b) High-altitude circulation forms at 500hPa, (c)(d) Skew-T diagrams for*  
38 *Lanzhou Zhongchuan Airport. The triangular marker indicates the location of*  
39 *Lanzhou Zhongchuan Airport.*

40 From July 3rd to 5th, 2022, a severe convective event occurred near  
41 Zhongchuan Airport. Figure S1(a) and (b) depict the geopotential height and  
42 temperature fields at 500hPa on July 3, 2022, at 08:00 (before convective  
43 development) and on July 4, 2022, at 08:00 (during convective development).  
44 Before convective initiation, there was a closed cold low-pressure center near the  
45 Caspian Sea. The system of two troughs and two ridges in the East Asia region  
46 shifted eastward. The low-pressure trough at the location of Zhongchuan Airport  
47 deepened, and there was a distinct cold outflow ahead of the trough. Figures S1(c)-  
48 (d) present Skew-T diagrams for the Zhongchuan Airport area in Lanzhou. On July  
49 3rd at 08:00, only Convective Inhibition (CIN) was observed without Convective  
50 Available Potential Energy (CAPE), indicating the presence of convective inhibition

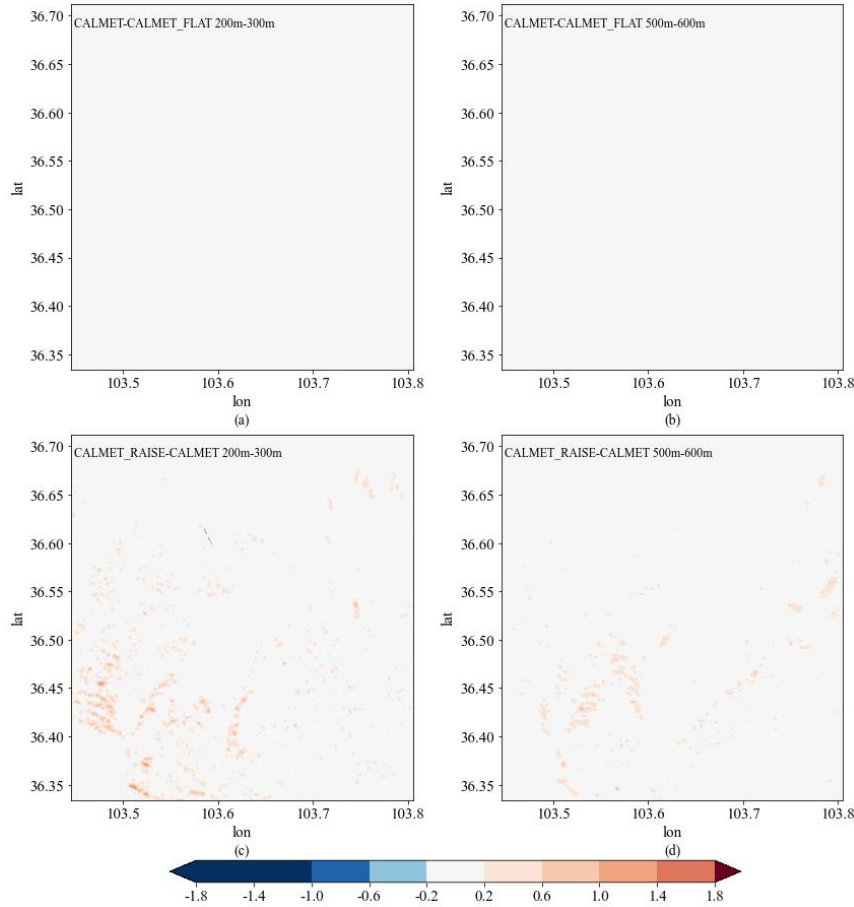
51 in the atmosphere, with insufficient available energy to support robust convective  
52 development. On July 4th at 08:00, there was CAPE from 620hPa to 300hPa, with a  
53 numerical value of 285.652 J/kg, and CIN is 111.712 J/kg. A situation where CAPE  
54 exceeded CIN is generally favorable for convective development. A higher CAPE  
55 value suggested sufficient potential convective energy in the atmosphere,  
56 supporting the development of convective clouds. Larger CAPE values were typically  
57 associated with more intense convection.

#### 58 4. Supplementary material



59

60 *Figure S2: Difference of 30m-10m altitude layer VWS of three experiments at*  
61 *19:00 on July 3, 2022 :(a):CALMET-CALMET\_FLAT; (b):CALEMT\_RAISE-CALMET; The*  
62 *red triangle is where the maximum value occurs, and the greentriangle is where the*  
63 *minimum value occurs.*



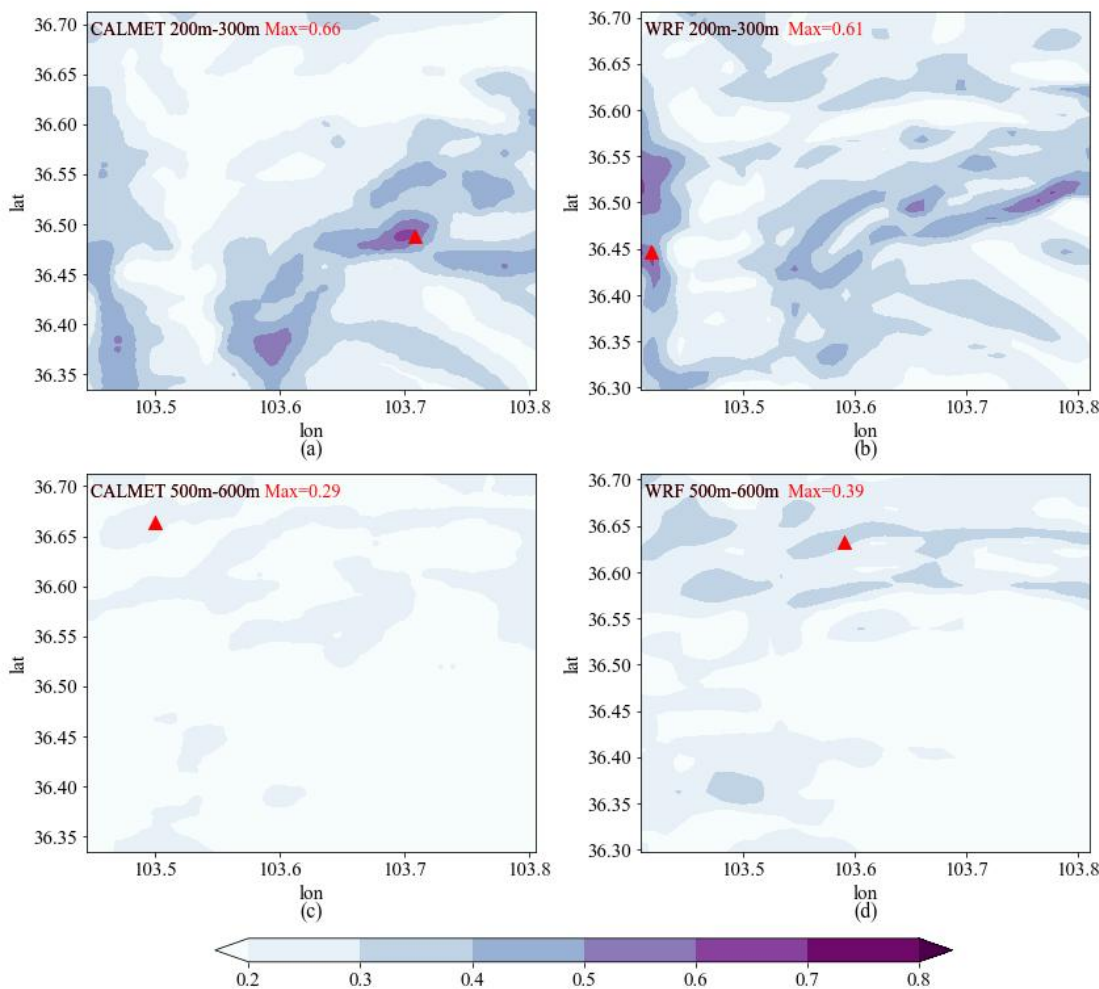
64

65 *Figure S3. VWS difference of three experiments at 19:00 on July 3,*  
 66 *2022 :(a),(b):CALMET-CALMET\_FLAT; (c),(d):CALEMT\_RAISE-CALMET; (a),(c):200m-*  
 67 *300m;(b),(d):500m-600m.The red triangle is where the maximum value occurs, and*  
 68 *the green triangle is where the minimum value occurs.*

69 To visually illustrate the differences among the three experiments and observe  
 70 the conditions at different height levels, Figure S2 and Figure S3 presents the VWS  
 71 differences for the three experiments at 19:00 on July 3, 2022. Analyzing the  
 72 difference between CALMET and CALMET\_FLAT, it is evident that in the 10m-30m  
 73 height range, CALMET's VWS values are significantly higher in the southeast  
 74 compared to CALMET\_FLAT, with minor differences in other locations. In the 200m-  
 75 300m and 500m-600m height ranges, the disparity between the two is minimal.

76 Examining the difference between CALMET\_RAISE and CALMET, in the 10m-  
 77 30m height range, CALMET generally has slightly higher values than CALMET\_RAISE.  
 78 Notably, in the southeast, CALMET exhibits a pronounced high-value area compared  
 79 to CALMET\_RAISE, with a maximum difference of 2.72 m/s/10m. Conversely, in the  
 80 central region, CALMET\_RAISE shows several high-value point-shaped areas  
 81 compared to CALMET, with the maximum exceeding CALMET by 2.96 m/s/10m. In  
 82 the 200m-300m height range, there are small, distinct high-value areas in the  
 83 southwest, with a maximum of 1.3 m/s/10m and a minimum of 0.22 m/s/10m.

84 Overall, CALMET\_RAISE's enhancement is more pronounced than its reduction. In  
 85 the 500m-600m height range, similar to the 200m-300m range, CALMET\_RAISE's  
 86 enhancement is more noticeable than the reduction, but the absolute value of the  
 87 difference decreases with increasing height.



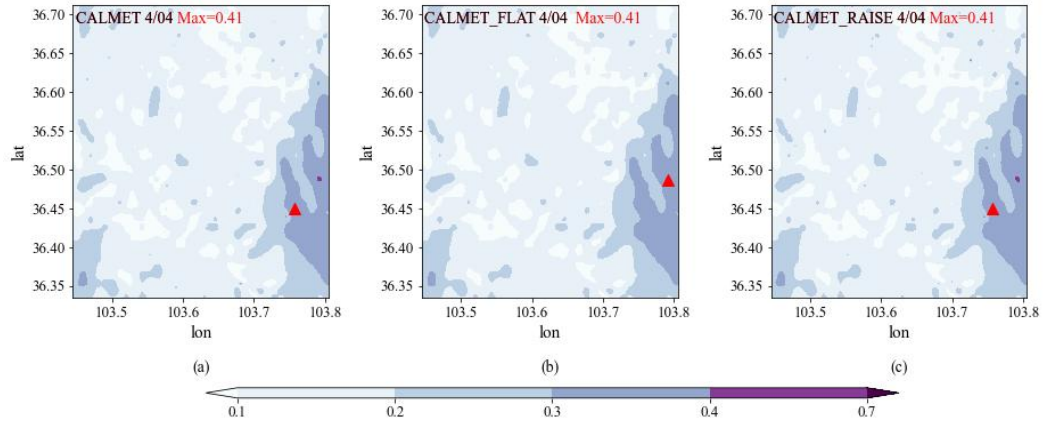
88

89 *Figure S4. VWS at 16:00 on July 3, 2022 (unit: m/s/10m). (a),(c)CALMET;*  
 90 *(b),(d)WRF; (a),(b): 200-300m VWS; (c),(d) VWS of 500m to 600m indicates the*  
 91 *location where the maximum value occurs.*

92 In the 200m-300m height layer (Figure S4(a),(b)), the maximum VWS values  
 93 simulated by both models are similar. CALMET's distribution trend is similar to that  
 94 of the 10m-30m layer: low values are observed on ridges and in northern  
 95 mountainous areas, while high values are distributed on the western slopes of the  
 96 ridges and in valley areas. WRF's maximum VWS values appear on the western  
 97 slopes of the ridges, with an overall irregular distribution. In the 500m-600m height  
 98 layer (Figure S4(c),(d)), CALMET's maximum VWS values are generally lower than  
 99 those of WRF, with instances where CALMET's values are lower than WRF's.

100





101

102 *Figure S5. 10m-30m VWS of CALMET(a), CALMET\_FLAT(b) and CALMET\_RAISE(c)*  
 103 *at 04:00 on July 4, 2022 (unit: m/s/10m). The triangle represents where the maximum*  
 104 *value occurs*

105 The strong agreement in maximum Vertical Wind Shear (VWS) values among  
 106 the three experiments during early morning and morning hours is evident. Taking  
 107 the VWS distribution at 04:00 on July 4 (Figure S5) as an example, the ground-level  
 108 VWS (10m-30m) shows consistent patterns across all three experiments, with  
 109 maximum values consistently located in the flat river valley to the east. This  
 110 indicates minimal terrain impact on VWS simulation by the CALMET model during  
 111 these time periods.

112 Valley winds typically influence VWS significantly over complex mountainous  
 113 terrain. However, in flat river valley areas, observed in these experiments, terrain  
 114 changes are minimal, exerting little influence on VWS. This suggests the model  
 115 accurately reflects atmospheric motion in flat regions, boosting confidence in VWS  
 116 distribution.